Long-range ordering in β-Cu-Zn-Al: Experimental and theoretical study

F. Lanzini,[1,2,*] R. Romero,[1,3] M. Stipcich,[1,2] and M. L. Castro[1,2]

[1]*Instituto de Física de Materiales Tandil (IFIMAT), Facultad de Ciencias Exactas, Universidad Nacional del Centro de la Provincia de Buenos Aires, Pinto 399 (B7000GHG) Tandil, Buenos Aires, Argentina*

[2]*Consejo Nacional dc Investigaciones Cientifícas y Técnicas (CONICET), Av. Rivadavia 1917, (C1033AAJ) Buenos Aires, Argentina*

[3]*Comisión de Investigaciones Científicas de la Provincia de Buenos Aires (CICPBA), Calle 526 e/10 y 11, (B1906APP) La Plata, Argentina*

(Received 14 November 2007; revised manuscript received 29 February 2008; published 30 April 2008)

We present the order-disorder transition temperatures for bcc Cu-Zn-Al shape-memory alloys measured by means of calorimetric and resistometric techniques. The investigation includes the line of compositions $Cu_{0.76-x/2}$-Zn_x-$Al_{0.24-x/2}$ $(0 \leqslant x \leqslant 0.48)$, i.e., the line with a constant conduction electron per atom ratio, $e/a = 1.48$. Experimental results are confronted with Monte Carlo simulations based on the Blume–Emery–Griffiths Hamiltonian. A set of exchange energies in first and second neighbors is calculated, which allows in close agreement reproduction of the experimental phase diagram.

DOI: 10.1103/PhysRevB.77.134207 PACS number(s): 64.60.Cn, 64.70.K−, 05.10.Ln

I. INTRODUCTION

Cu-based alloys are Hume–Rothery materials for which the stability of different phases at different compositions and temperatures mainly depends on the average number of conduction electrons per atom, or the electron to atom ratio (e/a).[1] At $e/a \approx 1.5$ and high temperatures, these alloys display a bcc structure (β phase). In general, at lower temperatures, the β phase is not a stable one and decomposition to stable phases takes place. However, the β phase can be retained below its stability limit by means of a suitable thermal treatment (quenching). During the cooling, this metastable phase can suffer one or two ordering transitions. Besides, depending on composition, these alloys are able to undergo a diffusionless, first-order, structural transition known as the martensitic transformation. Within Cu-based systems, the ternary Cu-Zn-Al alloy is one of the most studied, and it is worth mentioning that this alloy is very attractive because of its low cost and its very interesting properties such as shape memory, pseudoelasticity, and high damping power. These properties are directly associated with the martensitic transformation. Owing to the diffusionless nature of this phase transformation, the martensitic phase inherits the β phase atomic distribution; moreover, the martensitic transformation is strongly affected by the degree of chemical short- and long-range orderings developed in the alloy. In addition to the fundamental interest, this is one of the reasons for the investigation of the ordering transition in Cu-based shape-memory alloys.[2–4]

For the Cu-Zn-Al system, the stability range of the β phase decreases with decreasing temperature and centers around an electron concentration of ≈ 1.48. For this electron concentration, the β phase Cu-Zn alloy is stable at room temperature, while 840 K is the reported lower limit temperature for the Cu-Al β phase stability.[5,6] Below this temperature, the β phase decomposes into equilibrium phases α [fcc-(Cu)] and γ (complex cubic).

The present work is devoted to a detailed investigation of the order-disorder transition of the β phase of Cu-Zn-Al at fixed $e/a = 1.48$, i.e., $Cu_{0.76-x/2}$-Zn_x-$Al_{0.24-x/2}$, in the entire composition range $(0 \leqslant x \leqslant 0.48)$. Beforehand, this system has been studied for a limited composition range $(0.08 < x < 0.28)$ and has been shown that, in this range, the relative stability of the different ordered phases can be depicted as follows:[7] At high temperature, the equilibrium bcc β phase is disordered or short-range ordered (structure $A2$). Two types of long-range ordered (lro) structures can form as the temperature decreases: the $B2$ superlattice, which is formed by an ordering reaction between nearest neighbor (nn) pairs, and the $L2_1$ structure obtained by further ordering between next nearest neighbor (nnn) atoms.

For a suitable description of the different ordered structures, the general bcc lattice is divided into four fcc sublattices (I–IV), as shown in Fig. 1. The degree of lro is usually written in terms of the occupation probabilities p_A^k for an A atom to be placed at a site on sublattice k. The disordered state $A2$ is characterized by the fact that any atomic species A has the same probability to occupy any of sublattices I–IV, that is,

$$p_A^{\mathrm{I}} = p_A^{\mathrm{II}} = p_A^{\mathrm{III}} = p_A^{\mathrm{IV}} = c_A, \tag{1}$$

where c_A is the atomic concentration of element A.

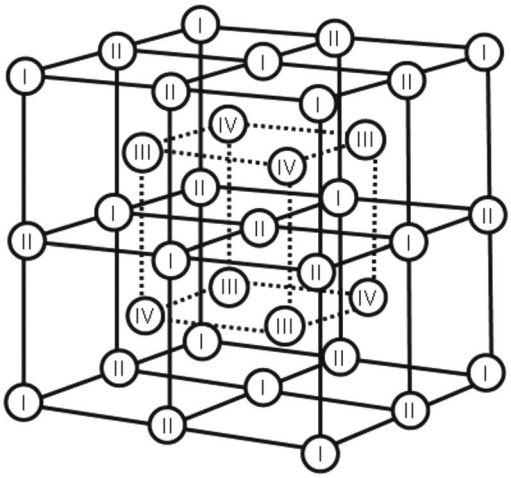

FIG. 1. General bcc lattice and the four fcc sublattices in which it is divided.

State $B2$ is characterized by

$$p_A^{\mathrm{I}} = p_A^{\mathrm{II}} \neq p_A^{\mathrm{III}} = p_A^{\mathrm{IV}}, \tag{2}$$

and the $L2_1$ order is characterized by

$$p_A^{\mathrm{I}} = p_A^{\mathrm{II}} \neq p_A^{\mathrm{III}} \neq p_A^{\mathrm{IV}} \neq p_A^{\mathrm{I}}. \tag{3}$$

Another ordered structure in nnn will be discussed in the course of this work, namely, the DO_3 structure, which is defined by the probabilities

$$p_A^{\mathrm{I}} = p_A^{\mathrm{II}} = p_A^{\mathrm{III}} \neq p_A^{\mathrm{IV}}. \tag{4}$$

For a ternary alloy, only six of the p_A^k are independent variables. For convenience, six long-range order parameters could be defined:[8,9]

$$x_A = \frac{p_A^{\mathrm{I}} + p_A^{\mathrm{II}} - p_A^{\mathrm{III}} - p_A^{\mathrm{IV}}}{4},$$

$$y_A = \frac{p_A^{\mathrm{I}} - p_A^{\mathrm{II}}}{2},$$

$$z_A = \frac{p_A^{\mathrm{III}} - p_A^{\mathrm{IV}}}{2} \tag{5}$$

(A=Cu or Zn).

Thus, for $A2$, $x_A = y_A = z_A = 0$; for $B2$ order, $x_A \neq 0$ and $y_A = z_A = 0$; and for $L2_1(DO_3)$, $x_A \neq 0$, $y_A = 0$, and $z_A \neq 0$.

To deal with ordering phenomena, the energy is usually expressed in terms of the exchange energies $W_{XY}^{(k)} = V_{XX}^{(k)} + V_{YY}^{(k)} - 2V_{XY}^{(k)}$, where the $V_{XY}^{(k)}$ represents the bond energies between atoms of species X and Y placed at a distance corresponding to kth neighbors. The values of such exchange energies determine the behavior of the alloy: for $W_{XY}^{(k)} > 0$, species X and Y tend to order in the kth neighborhood, whereas $W_{XY}^{(k)} < 0$ represents a tendency to segregate. For practical calculations, it is generally assumed that all the exchange energies vanish beyond some definite, small value of k. In this work, only interactions up to second neighbors will be taken into consideration.

Beyond the pioneer work of Rapacioli and Ahlers,[7] at least two important questions remain unsolved up to date. First, the behavior of the system as the Zn content is reduced is not clear: from the measurements made for Zn contents higher than around 8 at. %, it seems that both lines of order transitions ($A2 \leftrightarrow B2$ and $B2 \leftrightarrow L2_1$) tend to join for lower Zn contents.[7] In particular, for the limiting binary Cu-Al, contradictory results have been published;[10–13] one or two ordering reactions have been reported. The second main question still unsolved refers to the possibility of reproducing the experimental phase diagram by means of suitable theoretical calculations. Even when some work in this direction has already been done,[7,14] the results obtained do not seem to be completely satisfactory when the overall phase diagram is taken under consideration. The major aim of the present work is to find responses to these questions. In order to do so, the order-disorder transitions in $Cu_{0.76-x/2}$-Zn_x-$Al_{0.24-x/2}$ for $0 \leqslant x \leqslant 0.48$, shape-memory alloys have been experimentally determined by means of calorimetric and resistometric techniques. By performing Monte Carlo simulations within the Blume–Emery–Griffiths model, a set of constant exchange energies up to second neighbors that reproduces in close agreement the experimental results was deduced.

This paper is organized as follows. In Sec. II, we briefly describe the experimental method and the experimental results are presented. Section III is devoted to a discussion of the nature of the measured ordering reactions and in Sec. IV, we present details about the way that Monte Carlo simulations were performed, the results obtained, and their discussion. Finally, conclusions are outlined in Sec. V.

II. EXPERIMENT

A. Experimental techniques

The alloys were fabricated by melting 99.999% purity metals in sealed quartz tubes under a partial Ar atmosphere. Single crystals were grown in sealed quartz tubes in the usual way by the Bridgman method. The alloy compositions were determined from the starting masses of the constituent metals. The nominal compositions are given in Table I.

The transition temperatures were determined by electrical resistivity (ER) and differential scanning calorimetry (DSC) measurements taken during cooling from 1073 K to room temperature.

For the measurements of electrical resistivity, 15 mm long and 1.5×1.5 mm^2 cross-section samples were used. The electrical resistivity was monitored by using a standard four-point probe technique. The leads and a chromel-alumel thermocouple were spot welded to the sample. A Keithley 220 constant current generator was used to drive a current of 100 mA through the sample. A Keithley 186 nanovoltmeter measured the potential drop across the sample. The samples were annealed for 1 h at 1073 K before the run down in temperature starts. The experimental cooling rate has been chosen to be fast enough to avoid decomposition into the equilibrium phases. An order-disorder transition could be detected as a change in the slope of the resistivity-temperature curve.[15] As an example of the experimental measurements, we have shown in Fig. 2 the variation in electrical resistivity ρ against temperature during a cooling procedure for several compositions. The derivatives $d\rho/dT$ are also shown (insets).

Calorimetric measurements were carried out in a commercial DSC. The calorimetric runs were performed in the following way: From room temperature, samples were heated up to 920 K at 20 K/min; after being maintained for 1 min at 920 K, they were cooled down to room temperature at different rates, which are between 1 and 50 K/min. The samples were 1–1.5 mm high and 100–200 mg disks. Typical calorimetric curves are shown in Fig. 4.

B. Experimental results

As indicated previously, the β phase is stable, in general, at high temperatures. For the family of alloys studied in this work, the lower temperature of stability of this phase strongly depends on composition. Below this temperature, the β phase is no longer stable and decomposes into equilibrium phases α (fcc) and γ (complex cubic). In a previous

TABLE I. Nominal compositions of the different alloys investigated in the line $Cu_{0.76-x/2}$-Zn_x-$Al_{0.24-x/2}$ $(0 \leqslant x \leqslant 0.48)$ with constant conduction electron per atom ratio $e/a=1.48$, and measured ordering temperatures in K. The last column indicates the experimental technique used for the measurement: DSC: differential scanning calorimetry, ER: electrical resistometry.

x	$T_{A2\rightarrow B2}$	$T_{B2\rightarrow L2_1}$	$T_{A2\rightarrow L2_1/DO_3}$	Technique
0[a]			807	DSC
0.025			774.7	DSC
0.05			774.7	DSC
0.05			773	ER
0.1137	779	727		ER
0.1148	782.4	694.3		DSC
0.1217	803.6	696.8		DSC
0.1217	779	700		ER
0.1336	814.9	676		DSC
0.1336		667		ER
0.1534	798.9	648		DSC
0.1534	810	660		ER
0.1573	818.9	640.3		DSC
0.1613	811.5	634.9		DSC
0.1852	818	593		ER
0.1852	826.2	596.4		DSC
0.2169	834.5	534.5		DSC
0.2169	828	503		ER
0.2407	828	490		ER
0.2407	841.8	500		DSC
0.2526	818	480		ER
0.2685	833	430		DSC
0.2804	833	444		ER
0.38	803			ER
0.48	727.8			DSC
0.48	726			ER

[a]See Ref. 16.

work, it has been found that the tendency to decomposition is higher as the Al content is higher.[17] In particular, for those alloys richer in aluminium (small x), we found that the β phase is not stable at the temperatures at which ordering should take place. Thus, during a cooling measurement, the precipitation of stable phases almost inhibits the occurrence of the ordering transitions. This difficulty can be overrun by choosing sufficiently fast cooling rates for the measurements: in this way, it is possible to suppress the precipitation of stable phases, retaining the β phase in a metastable state. An example of this procedure can be viewed in Fig. 3, where a set of DSC curves obtained for the $x=0$ alloy at cooling rates of 5, 10, 20, 30, and 40 K min^{-1} is shown. For slow cooling rates, decomposition of the β phase in the stable structural phases inhibits the order transitions. However, for cooling rates higher than 20 K min^{-1}, an exothermic peak at a temperature near 807 K can be observed; as the cooling rates increase, the peak turns more evident. This strongly suggests that the signal corresponds to an ordering reaction and not to

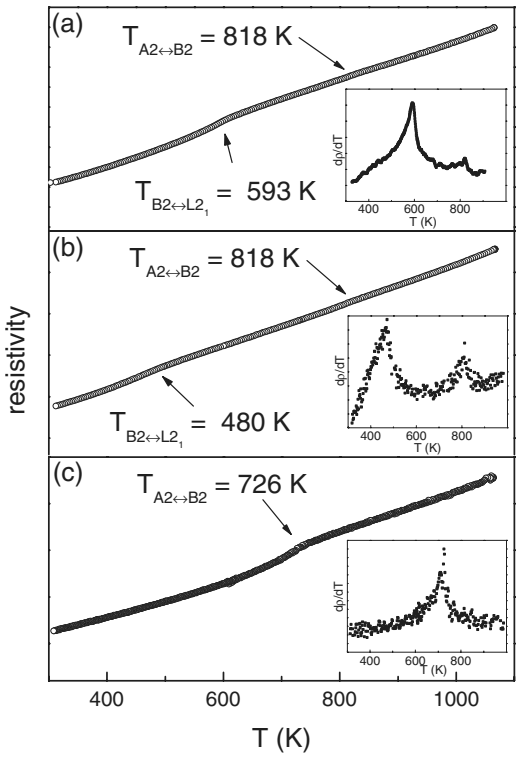

FIG. 2. Variation in the electrical resistivity and its derivative (insets) for several alloys as a function of temperature during cooling. (a) $x=0.1852$, (b) $x=0.2526$, and (c) $x=0.4800$.

decomposition of the β phase. For this alloy, additional measurements were made by means of electrical resistometry in a range of temperatures above the upper limit of operation of our DSC. This experiment allows discarding of the existence of additional ordering reactions at higher temperatures. For the alloys with $x=0.025$ and $x=0.05$, analogous experimental care was taken: several calorimetric runs with different cooling rates were made in order to separate the signal due to atomic ordering from that arising from decomposition. At

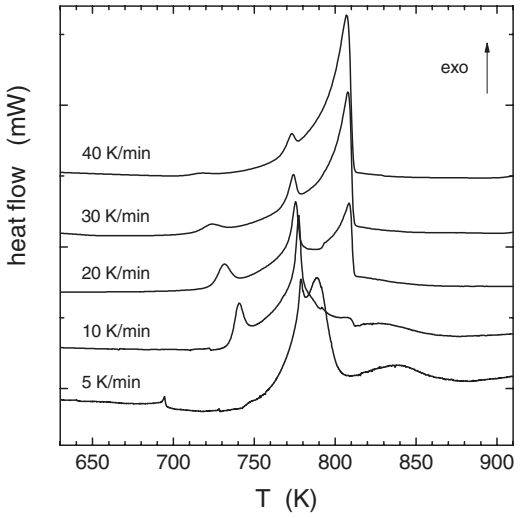

FIG. 3. DSC measurements for $x=0$ at different cooling rates, as indicated in the figure.

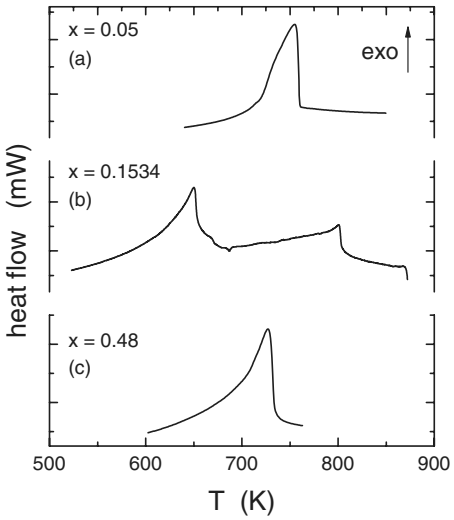

FIG. 4. DSC measurements for Cu-Zn-Al with compositions as indicated in the figure.

intermediate compositions in the range $0.1137 \leqslant x \leqslant 0.2804$, two ordering reactions were observed [Figs. 2(a) and 2(b), Fig. 4(b)]. The separation in temperature between these transitions increases with the Zn content. Whereas the high temperature transition shows a small dependence on composition, the lower one rapidly decreases as the Zn content is raised. Simultaneously, the detection of this last transition turns more difficult. This difficulty is not only attributable to experimental reasons but there are physical impediments in order that the ordering process completely can take place: owing to the relatively low thermal energy available, the migration-aided atomic exchanges hardly occur. Thus, beyond $x=0.2804$, only the high temperature transition could be detected.

In Table I and Fig. 5, we present the measured ordering temperatures. The overall experimental findings could be roughly depicted as follows: whereas for Zn content lower than or equal to 5 at. % ($0 \leqslant x \leqslant 0.05$) only one order transition was observed, for intermediate compositions ($0.1137 < x < 0.2804$), two order transitions can be detected. With further increasing the Zn content ($0.2804 \leqslant x \leqslant 0.48$), again a

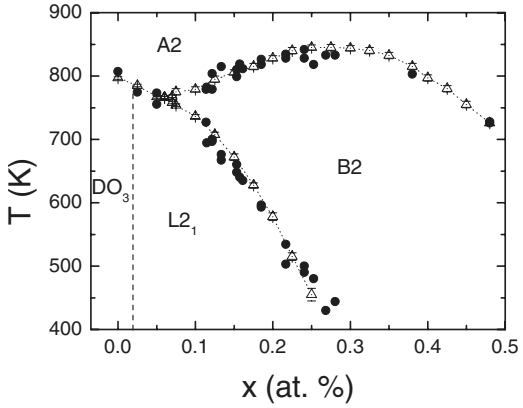

FIG. 5. Measured order-disorder temperatures (black dots) and results of the calculations (hollow triangles). The dotted lines are guides to the eyes.

single transition was observed. In Table I, the transition temperatures were classified according to the ordered phases involved. Consequently, $T_{A2\rightarrow B2}$ designates the temperature where a transition from a disordered high temperature $A2$ phase to a low temperature $B2$ phase occurs. Notwithstanding that the experimental techniques used in this work do not provide direct information on the nature of the different phases involved, the justification for our classification will become clear below.

III. DISCUSSION

A. Nature of the ordering transitions

As has been pointed out before, there is some discrepancy in the literature about the number of order-disorder transitions in Cu-Al with compositions near Cu_3Al ($x \approx 0$ alloys). Whereas some authors[10,11,18] support the idea that two separate ordering reactions, $A2 \rightarrow B2$ and $B2 \rightarrow DO_3$, occur, others[12,13,19] propose the existence of a single $A2 \rightarrow DO_3$ transition. This discrepancy may be attributed to the difference in the experimental conditions that the measurements have been performed in. The present experimental data seem to confirm the second hypothesis: whereas the reported $T_{A2\leftrightarrow B2}$ is about 973 K,[10] careful measurements made in this work by means of electrical resistometry techniques in the range between 1173 and 773 K do not show evidence of this order transition. Anyhow, it is a well-established fact that the low temperature phase is DO_3. Thus, the single ordering reaction we found at $T=807$ K for the alloy with $x=0$ necessarily represents a transformation from a high temperature $A2$ state to a DO_3 structure. Figure 3 shows the characteristic profile for this transition (thermograms corresponding to cooling rates of 20 K min^{-1} and higher). As can be seen, the associated calorimetric peak is very sharp, this is an indication that the kinetics of the transition is first order. Also, for the alloys with $x=0.025$ and $x=0.05$, the single calorimetric peak detected has to be associated with an $A2 \rightarrow DO_3$ (or $L2_1$) transition. The reason for such hypothesis becomes clear when analyzing the overall experimental information as shown in Fig. 5. The calorimetric signals associated with these reactions keep the typical shape of a first-order transition [Fig. 4(a)]. On the other hand, for alloys with $0.1137 \leqslant x \leqslant 0.2804$, two ordering transitions were observed. It has been shown that, in this composition range, ordering proceeds in two steps, $A2 \rightarrow B2$ and $B2 \rightarrow L2_1$.[7,20] Besides, the critical temperatures determined in the present work agree with those previously reported in Ref. 7. It is worth mentioning that the λ shape of the corresponding DSC peaks supports the idea that both ordering reactions have a continuous character [Fig. 4(b)]. Finally, the measurement made on the binary $x=0.48$ alloy gives a transition temperature near 727 K [Fig. 4(c)]. This reaction is well known to arise from the disordered state $A2$ to one ordered in next neighbors $B2$ in a continuous way.[21]

B. Monte Carlo simulations

1. Details of the simulations

In order to gain insight into the physical phenomena that govern the relative stability of the different ordered phases,

we were encouraged to resort to some model that correctly reproduces the experimental data. Several methods with different degrees of approximation and complexity can be used to deal with ordering phenomena: both analytical approaches, such as the simplest Bragg–Williams–Gorski approximation (BWGA) and the more elaborated cluster variation method, or purely numerical techniques, such as Monte Carlo simulations.[22,23] Attempts made to fit the experimental order-disorder temperatures shown in Fig. 5 with the expressions derived in the BWGA (Ref. 8) were unsuccessful, so it was necessary to appeal to a more powerful method. We opted to perform Monte Carlo simulations:[24–26] this method has the advantage that, in principle, it gives the correct phase diagram for a given model Hamiltonian. The Blume–Emery–Griffiths (BEG) Hamiltonian[27,28] is equivalent to a pair interaction model for a ternary alloy (see the Appendix) and is then the natural choice for our problem. The BEG Hamiltonian is constructed as follows: a pseudospin variable σ_i with three possible values (orientations) is associated with each atomic site; $\sigma_i=+1$, 0, or -1 depending on the site i occupied with a Cu, Zn, or Al atom. The internal energy of the alloy when considering interactions in first and second neighbors can be written as

$$H = \sum_{\langle ij \rangle}^{nn} \{J_1 \sigma_i \sigma_j + K_1 \sigma_i^2 \sigma_j^2 + L_1(\sigma_i \sigma_j^2 + \sigma_i^2 \sigma_j)\} + \sum_{\langle ij \rangle}^{nnn} \{J_2 \sigma_i \sigma_j + K_2 \sigma_i^2 \sigma_j^2 + L_2(\sigma_i \sigma_j^2 + \sigma_i^2 \sigma_j)\}, \quad (6)$$

where the first sum is extended over all the nn pairs and the second one over the nnn. The quantities $J_{1(2)}$, $L_{1(2)}$, $K_{1(2)}$ are linear combinations of the exchange energies (see the Appendix):

$$J_k = \frac{W_{\mathrm{CuAl}}^{(k)}}{4},$$

$$K_k = \frac{2W_{\mathrm{CuZn}}^{(k)} + 2W_{\mathrm{ZnAl}}^{(k)} - W_{\mathrm{CuAl}}^{(k)}}{4},$$

$$L_k = \frac{W_{\mathrm{CuZn}}^{(k)} - W_{\mathrm{ZnAl}}^{(k)}}{4},$$

$$k = 1,2. \quad (7)$$

In what follows, our results will be discussed in terms of the $W_{AB}^{(k)}$, which, as mentioned above, more clearly describes the tendency to ordering or segregation.

Simulations were carried out in a bcc computer crystal with up to 2×64^3 atomic sites under periodic boundary conditions. The initial distribution of the atomic species over the lattice was chosen either completely random in order to simulate cooling processes or with the maximum degree of order compatible with composition to perform equivalent heating processes. For a fixed value of the temperature T, the lattice was sequentially covered, deciding the exchange between two nn atoms by the usual Metropolis criterion;[29] the energy difference involved in the atomic exchange being evaluated through the BEG Hamiltonian, Eq. (6). For a given temperature and composition, the number of Monte Carlo steps (MCSs) (exchange attempts per site) required to reach the equilibrium was performed; the order parameters defined in Eq. (2) were evaluated at each MCS. After the system reaches equilibrium, the simulation continues in order to obtain averages of the equilibrium order parameters with the desired accuracy; the total number of MCSs performed varies, according to temperature, in the range $2.5 \times 10^4 - 2.5 \times 10^5$. Then, the temperature was increased (or decreased) in discrete jumps, and the simulation continued until the new state of equilibrium was reached. The start of an ordering reaction was detected by analyzing the change in the order parameters (see Fig. 6).

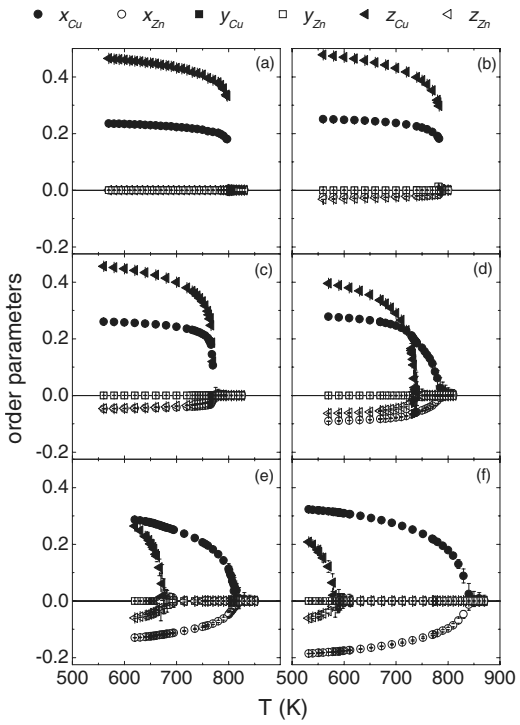

FIG. 6. Evolution of the order parameters against temperature for (a) $x=0$, (b) $x=0.025$, (c) $x=0.05$, (d) $x=0.1$, (e) $x=0.15$, and (f) $x=0.2$.

2. Results of the simulations

The main objective of the simulations was to find numerical values for the six exchange energies in order to obtain the best agreement possible with the experimental data. In the first stage, we adopt the values of the exchange energies for Cu-Zn proposed by Inden:[9] $W_{\mathrm{CuZn}}^{(1)}=955K_B$ and $W_{\mathrm{CuZn}}^{(2)}=535K_B$. These energies accurately reproduce the measured transition temperature in the $x=0.48$ alloy (Table I). In order to calculate the remaining four exchange energies, a mechanism of successive approximations was used. In the first stage, two trial values for the exchange energies of the Cu-Al pairs were taken; these values were chosen in such a way that they reproduce the measured transition temperature for the binary Cu-Al ($x=0$), $T_{A2 \leftrightarrow DO_3} \approx 807$ K. Then, the exchange energies of the Zn-Al pairs were calculated by adjusting them until the measured transition temperatures $T_{A2 \leftrightarrow B2}$ and $T_{A2 \leftrightarrow L2_1}$ for an intermediate composition ($x=0.2169$)

TABLE II. Exchange energies obtained.

$W^{(1)}_{\mathrm{CuAl}}=1660K_B$	$W^{(2)}_{\mathrm{CuAl}}=920K_B$
$W^{(1)}_{\mathrm{ZnAl}}=-45K_B$	$W^{(2)}_{\mathrm{ZnAl}}=285K_B$
$W^{(1)}_{\mathrm{CuZn}}=955K_B$	$W^{(2)}_{\mathrm{CuZn}}=535K_B$

were reproduced. Subsequent corrections were made by iteratively readjusting the energies of Cu-Al to reproduce the data for the $x=0.115$ alloy and then recalculating the values for Zn-Al as before. This iterative procedure successfully converged to the set of exchange energies indicated in Table II. The corresponding phase diagram is shown in Fig. 5 and will be discussed in more detail below.

Several values for the exchange energies of the binary Cu-Al were previously reported. Rapacioli and Ahlers[7] obtained $W^{(1)}_{\mathrm{CuAl}}=1345K_B$ and $W^{(2)}_{\mathrm{CuAl}}=825K_B$ by using the BWGA. As one of the authors signaled later,[3] these values are not good enough to reproduce the measured ordering temperature for the $x=0$ alloy; a dependence on composition of the exchange energies was proposed. With data from the ternary Cu-Al-Mn, Prado *et al.*[11] obtained $W^{(1)}_{\mathrm{CuAl}}=1605K_B$ and $W^{(2)}_{\mathrm{CuAl}}=856K_B$. These values were also obtained within the BWGA, starting from the fact that the authors assumed two ordering reactions in Cu_3Al, which is in disagreement with the results reported in the present work. More recently, Obradó *et al.*[13] reported $W^{(1)}_{\mathrm{CuAl}}=1552K_B$ and $W^{(2)}_{\mathrm{CuAl}}=1008K_B$, which are consistent with the existence of only one ordering reaction for the $x=0$ alloy. These values were obtained by means of a procedure similar to that used in this work, fitting experimental transition temperatures for the Cu-Al-Mn ternary. The values we obtained for $W^{(1)}_{\mathrm{CuAl}}$ and $W^{(2)}_{\mathrm{CuAl}}$ are in the range of these previously reported, the first one being somewhat higher. As can be seen from the values shown in Table II, the exchange energies for Zn-Al pairs are very low. This is an indicative of the scarce tendency to ordering between both atomic species, as can be observed in the phase diagram of the binary subsystem.[5] The Cu-Zn is probably the best known of the three binary subsystems. Our results show that the values for the exchange energies reported by Inden[9] are good enough in order to reproduce the experimental phase diagram even when aluminum is incorporated as a third alloying element.

Some ambiguity remains in the literature about the nature of the state ordered in the first and second neighbors for this family of alloys. Whereas agreement exists on the fact that the low temperature phase for Cu-Al is DO_3, some point exists where the structure becomes $L2_1$ when Zn is gradually incorporated as a third element.[30] As can be seen from the definitions in Eqs. (1)–(4), the difference between both ordered states is very subtle. With the aid of the energies obtained, some conclusions can be made about the distribution of the atomic species over the sublattices. As long as the exchange energies in the first neighbors are higher for the Cu-Al and Cu-Zn systems, a state with minimal energy when considering only interactions up to nn will consist of the Cu atoms full filling lattices I and II, the remaining atoms occupying the other two sublattices. If interactions in nnn are now considered, a rearrangement of the atomic species over sublattices III and IV occurs in order to maximize the number of second neighbors bonds between Cu and Al. This leads to the occupation of one of these sublattices (say, sublattice III) with the Cu atoms that remain after sites I and II were completely filled, and Al atoms occupy sublattice IV. Zn atoms complete sites III and IV. In the phase diagram presented in this work, the Cu contents vary from 76 at. % ($x=0$) in the Al-rich side to 52 at. % ($x=0.48$) in the Zn-rich side. When the Cu content is equal to or higher than 75 at. %, the three sublattices I–III will be filled with majority atoms. Following the definitions in Eqs. (1)–(4), this distribution corresponds to a DO_3 ordering. On the other hand, when the Cu content is lower than 75 at. %, some Zn remains, occupying III sites. The analysis of the occupation numbers leads to the conclusion that this kind of structure belongs, strictly speaking, to an $L2_1$ type. In terms of the Zn concentration, the change from DO_3 to $L2_1$ ground states occurs at $x=0.02$. This is indicated with a dashed line in Fig. 5.

By using the exchange energies listed in Table II within the BEG Hamiltonian [Eqs. (6) and (7)], the theoretical phase diagram shown in Fig. 5 was obtained. The transition temperatures, indicated with open triangles, were determined by evaluating the evolution of the order parameters [Eq. (5)] during cooling processes in simulation boxes containing $2\times L^3$ ($L=32$ or 64) atomic sites. Transition temperatures obtained for both values of L are, within the resolution of the simulations, almost coincident (differences rarely exceed 5 K); the error bars in Fig. 5 account for these small discrepancies. Additionally, a few detailed simulations were made, showing that the thermal evolution of the order parameters is in close agreement for both crystal sizes. These observations indicate that finite-size effects are not relevant for the present purposes.

The calculated phase diagram reproduces the essential features of the measured one quite well. In the low-Zn content of the phase diagram (small x), only one phase transition, from $A2$ to DO_3 ($L2_1$), is predicted. As the Zn content is increased up to $x\approx 0.07$, the transition splits into two separate stages: the upper in temperature corresponds to the transition $A2\leftrightarrow B2$ and the other to the $B2\leftrightarrow L2_1$ ordering. With further increment in the Zn content, $T_{A2\leftrightarrow B2}$ gradually increases until a maximum is reached near $x=0.3$ and then begins to decrease. On the other hand, $T_{B2\leftrightarrow L2_1}$ monotonically decreases up to $x=0.25$.

In Fig. 6, we show detailed calculations of the variation in order parameters close to the ordering temperatures for six representative values of x. There are notorious differences as the composition is varied. For low zinc contents [$x=0$, 0.025, and 0.05, Figs. 6(a)–6(c)], the $A2\leftrightarrow DO_3$ ($L2_1$) transition involves a discontinuity in the relevant order parameters; this indicates a first-order nature of the ordering reaction. This point of view is supported by the observation of metastable states at the critical temperature, giving place to typical two-step relaxation processes.[25,26] In contrast, at the $A2\leftrightarrow B2$ transition occurring for higher zinc contents, the order parameters vanish in a continuous manner, indicating a continuous character of the transition. This is also the case for the $B2\leftrightarrow L2_1$ transition [Figs. 6(d)–6(f)].

IV. SUMMARY AND CONCLUSIONS

In this work, we have determined the order-disorder temperature in a wide range of compositions for the ternary alloy

β-Cu-Zn-Al with a constant electronic concentration $e/a=1.48$. The measurements were made by using two experimental techniques: differential scanning calorimetry and electrical resistometry. The results obtained indicate that, whereas for intermediate compositions two continuous ordering reactions, $A2 \rightarrow B2$ and $B2 \rightarrow L2_1$, exist, in the Al-rich side, both transitions join into a single first-order reaction, $A2 \rightarrow L2_1$ (DO_3). We found that the experimental results can be reproduced in close agreement by means of Monte Carlo simulations by using a Hamiltonian that includes up to second neighbor constant interactions. A set of exchange energies (Table II) was obtained by fitting to the experimental data. Simulations predict that the point where the ordering transition $A2 \rightarrow L2_1$ (DO_3) splits into two transitions occurs for a Zn content near about $x=0.065-0.070$. This finding agrees with the experimental information available. The nature of the transitions was discussed. The Monte Carlo simulations reproduce the ordering temperatures and its kinetic features. A simple criterion to decide whether the state ordered up to next nearest neighbors is DO_3 or $L2_1$ is proposed. According to this criterion, the low temperature ordered state is DO_3 up to $x=0.02$ and $L2_1$ for higher Zn contents.

ACKNOWLEDGMENTS

This work was supported by the Consejo Nacional de Investigaciones Científicas y Técnicas, Comisión de Investigaciones Científicas de la Provincia de Buenos Aires, and Secretaría de Ciencia y Técnica of the Universidad Nacional del Centro.

APPENDIX: BLUME–EMERY–GRIFFITHS HAMILTONIAN

The internal energy of a lattice containing N atomic sites when we consider only interactions up to nearest neighbors can be expressed as

$$H^{(1)} = \sum_{i,j} V(i,j), \tag{A1}$$

where the sum extends over all nn pairs i, j and $V(i,j)$ is the bond potential between the atom placed at i and the one placed at j. For a ternary alloy with elements A, B, and C,

$$V(i,j) = \delta_{AA}^{ij} V_{AA}^{(1)} + \delta_{AB}^{ij} V_{AB}^{(1)} + \delta_{AC}^{ij} V_{AC}^{(1)} + \delta_{BC}^{ij} V_{BC}^{(1)} + \delta_{CC}^{ij} V_{CC}^{(1)},$$

where $V_{XY}^{(1)}$ is the interaction potential between atoms of species X and Y placed as nn. The δ_{XY}^{ij} takes the value 1 if site i is occupied with an X atom and site j with a Y atom (or vice versa), and the value 0 otherwise. Let us associate with each position i a pseudospin variable σ_i able to take one of the three values +1, 0, or −1 depending on the site i being occupied with an A, B, or C atom, respectively. The several δ_{XY}^{ij} can then be expressed as

$$\delta_{AA}^{ij} = \frac{1}{4}(\sigma_i^2\sigma_j^2 + \sigma_i^2\sigma_j + \sigma_i\sigma_j^2 + \sigma_i\sigma_j),$$

$$\delta_{AB}^{ij} = \frac{1}{2}(\sigma_i^2 + \sigma_j^2 + \sigma_i + \sigma_j - \sigma_i^2\sigma_j - \sigma_i\sigma_j^2 - 2\sigma_i^2\sigma_j^2),$$

$$\delta_{AC}^{ij} = \frac{1}{2}(\sigma_i^2\sigma_j^2 - \sigma_i\sigma_j),$$

$$\delta_{BC}^{ij} = \frac{1}{2}(\sigma_i^2 + \sigma_j^2 - \sigma_i - \sigma_j + \sigma_i^2\sigma_j + \sigma_i\sigma_j^2 - 2\sigma_i^2\sigma_j^2),$$

$$\delta_{CC}^{ij} = \frac{1}{4}(\sigma_i^2\sigma_j^2 - \sigma_i^2\sigma_j - \sigma_i\sigma_j^2 + \sigma_i\sigma_j).$$

Replacing this expression in Eq. (A1) and rearranging terms:

$$H^{(1)} = \frac{-2V_{AC}^{(1)} + V_{AA}^{(1)} + V_{CC}^{(1)}}{4} \sum_{i,j} \sigma_i\sigma_j + \frac{2V_{AC}^{(1)} - 4V_{AB}^{(1)} - 4V_{BC}^{(1)} + V_{AA}^{(1)} + V_{CC}^{(1)} + 4V_{BB}^{(1)}}{4} \sum_{i,j} \sigma_i^2\sigma_j^2$$
$$+ \frac{-2V_{AB}^{(1)} + 2V_{BC}^{(1)} + V_{AA}^{(1)} - V_{CC}^{(1)}}{4} \sum_{i,j} (\sigma_i^2\sigma_j + \sigma_i\sigma_j^2) + \frac{V_{AB}^{(1)} + V_{BC}^{(1)} - 2V_{BB}^{(1)}}{2} \sum_{i,j} (\sigma_i^2 + \sigma_j^2) + \frac{V_{AB}^{(1)} - V_{BC}^{(1)}}{2} \sum_{i,j} (\sigma_i + \sigma_j) + \frac{1}{2} V_{BB}^{(1)}.$$

The last three terms only depend on composition and can be neglected as long as we keep the composition constant. By remembering the definitions for the exchange energies ($W_{XY}^{(1)} = -2V_{XY}^{(1)} + V_{XX}^{(1)} + V_{YY}^{(1)}$) and identifying species A, B, and C with Cu, Zn, and Al, respectively, the factors that multiply the first three sums in the preceding expression can be easily identified with parameters J_1, K_1, and L_1, as defined in Eq. (6). Contributions to the energy arising from next nearest neighbor interactions lead to the inclusion of an $H^{(2)}$ term in an analogous fashion.

*flanzini@exa.unicen.edu.ar

[1] T. B. Massalki and U. Mizutani, Prog. Mater. Sci. **22**, 151 (1978).
[2] J. Elgueta, J. L. Macqueron, and A. Planes, J. Phys.: Condens. Matter **4**, 285 (1992).
[3] M. Ahlers, Prog. Mater. Sci. **30**, 135 (1986).
[4] A. Planes, R. Romero, and M. Ahlers, Acta Metall. Mater. **38**, 757 (1990).
[5] *Metals Handbook*, 8th ed. (American Society for Metals, Metals Park, OH, 1973).
[6] J. Miettinen, Metall. Mater. Trans. A **33A**, 1639 (2002).
[7] R. Rapacioli and M. Ahlers, Scr. Metall. **11**, 1147 (1977).
[8] G. Inden, Z. Metallkd. **66**, 577 (1975).
[9] G. Inden, Z. Metallkd. **66**, 648 (1975).
[10] J. Soltys, Phys. Status Solidi A **63**, 401 (1981).
[11] M. Prado, M. Sade, and F. Lovey, Scr. Metall. Mater. **28**, 545 (1993).
[12] M. Jurado, T. Castán, L. Mañosa, A. Planes, J. Bassas, X. Alcobé, and M. Morin, Philos. Mag. A **75**, 1237 (1997).
[13] E. Obradó, C. Frontera, Ll. Mañosa, and A. Planes, Phys. Rev. B **58**, 14245 (1998).
[14] S. C. Singh, Y. Murakami, and L. Delaey, Scr. Metall. **12**, 435 (1978).
[15] P. L. Rossiter, *The Electrical Resistivity of Metals and Alloys* (Cambridge University Press, Cambridge, 1987).
[16] The nominal composition of this alloy is Cu-24.4 at. % Al, i.e., this alloy does not exactly fall in the line of compositions $Cu_{0.76-x/2}-Zn_x-Al_{0.24-x/2}$. Anyhow, it is expected that this small departure from the required composition does not significantly modify the determined values of the interchange energies. For conciseness, we will refer to this alloy as $x=0$.
[17] M. L. Castro and R. Romero, Mater. Sci. Eng., A **273**, 577 (1999).
[18] R. Kainuma, N. Satoh, X. J. Liu, I. Ohnuma, and K. Ishida, J. Alloys Compd. **266**, 191 (1998).
[19] M. T. Ochoa-Lara, H. Flores-Zúñiga, D. Ríos-Jara, and G. Lara-Rodríguez, J. Mater. Sci. **41**, 4755 (2006).
[20] C. Satto, J. Jansen, C. Lexcellent, and D. Schryvers, Solid State Commun. **116**, 273 (2000).
[21] F. W. Jones and C. Sykes, Proc. R. Soc. London, Ser. A **161**, 440 (1937).
[22] F. Ducastelle, *Order and Phase Stability in Alloys* (North-Holland, Amsterdam, 1991).
[23] G. Inden and W. Pitsch, *Materials Science and Technology: A Comprehensive Treatment* (VCH, Weinheim, 1991), Vol. 5.
[24] K. Binder, Rep. Prog. Phys. **60**, 487 (1997).
[25] *Monte Carlo Methods in Statistical Physics*, edited by K. Binder (Springer-Verlag, Berlin, 1987).
[26] O. G. Mouritsen, *Computer Studies of Phase Transitions and Critical Phenomena* (Springer-Verlag, Berlin, 1984).
[27] M. Blume, V. J. Emery, and R. B. Griffiths, Phys. Rev. A **4**, 1071 (1971).
[28] D. Mukamel and M. Blume, Phys. Rev. A **10**, 610 (1974).
[29] N. Metropolis, A. W. Rosenbluth, M. N. Rosenbluth, A. H. Teller, and E. Teller, J. Chem. Phys. **21**, 1087 (1953).
[30] M. H. Wu and C. M. Wayman, Scr. Metall. Mater. **25**, 1635 (1991).